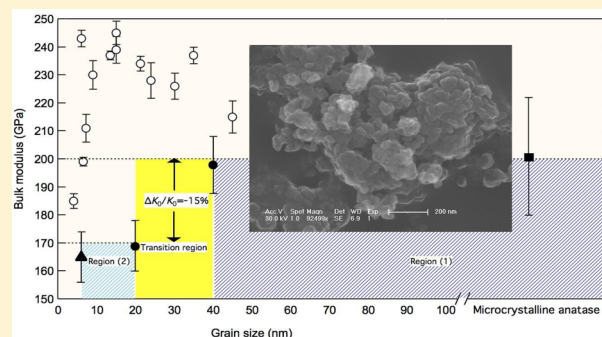


Compressibility of Nanocrystalline TiO₂ Anatase

Yahya Al-Khatatbeh,^{*,†,‡} Kanani K. M. Lee,[‡] and Boris Kiefer[§][†]Physics Department, Bard College at Simon's Rock, Great Barrington, Massachusetts 01230, United States[‡]Department of Geology and Geophysics, Yale University, New Haven, Connecticut 06511, United States[§]Department of Physics, New Mexico State University, Las Cruces, New Mexico 88003-8001, United States

ABSTRACT: Using high-resolution, synchrotron-based powder X-ray diffraction (XRD), we have studied the high-pressure behavior of the anatase phase of nanocrystalline TiO₂ (nc-TiO₂) under hydrostatic conditions. We find that for anatase with a grain size larger than ~40 nm, the room-pressure bulk modulus K_0 remains constant at ~200 GPa to within experimental uncertainties. An ~15% decrease in K_0 is observed for grains that are ~20 nm in size and remains unchanged for grains down to 6 nm in diameter, indicating a rapid increase in compressibility for nc-TiO₂ anatase between 40 and 20 nm.



INTRODUCTION

TiO₂ anatase is an important material in many technological applications including photocatalysis, ceramics, electronic storage media, and hydrogen storage applications.^{1–3} Due to its promising technological applications,^{1–3} the high-pressure behavior of nc-TiO₂ anatase has attracted great interest over the past decade^{4–17} with studies focusing on pressure-induced phase transitions and amorphization.^{5–7,9,11,12,14–17} However, little is known about the effect of particle size on the equation of state (EOS) of TiO₂ anatase and the few available studies are inconclusive and controversial: previous experiments on nc-TiO₂ anatase have found that the bulk modulus may increase or decrease with decreasing particle size.^{4,8,10,13} Some of the complications likely arise from the lack of hydrostaticity in the sample under pressure,^{8,10} whereas other studies do not provide the EOS of nc-TiO₂ anatase¹³ or have some important issues (e.g., typographical errors or mistakes in EOS determination) in the reported EOS and/or measured value of its zero-pressure volume V_0 .⁴ Thus, a consistent understanding of the behavior of nanocrystalline TiO₂ anatase as grain size is changed is presently lacking.

To eliminate, or at least reduce, the controversy regarding the grain size dependence, we study the size dependence of the bulk modulus in nc-TiO₂ anatase under hydrostatic conditions at pressures up to ~11 GPa. Therefore, this work along with a reanalysis of previous studies on nc-TiO₂ anatase^{4,8,10,13} allow us to reach consistency among several studies of the size dependence of the bulk modulus of nc-TiO₂ anatase.

EXPERIMENTAL METHODS

Nanocrystalline samples of 99% TiO₂ anatase/rutile powder (Nanostructured & Amorphous Materials, Inc., 50 nm average particle size) and 99.7% TiO₂ anatase powder (Alfa Aesar, 15 nm average particle size) were used as starting materials in our

diamond-anvil cell (DAC) experiments. We confirmed the grain sizes by using the full-width-half-maximum¹⁸ of the XRD peaks to be 40(±3) and 20(±4) nm, respectively, consistent with scanning electron microscope measurements which yielded particle sizes of ~40–60 and ~20–30 nm, respectively. We performed two independent room temperature, high-pressure DAC experiments to study the EOS of nc-TiO₂ anatase (Table 1). A mixture of methanol–ethanol–water (M-E-W) (16:3:1 by volume) was used as the pressure medium.¹⁹ For pressures up to ~11 GPa, M-E-W is hydrostatic.^{20,21} Rhenium and stainless steel gaskets of initial thicknesses of 270 μm were precompressed to thicknesses of 30 μm. The sample, pressure calibrant ruby,²² and pressure medium were placed in a 120 or 150 μm sample chamber in the center of the gasket and compressed between a pair of matched 300 μm culet diamonds. We collected angular-dispersive XRD at room temperature (Figure 1) using a MAR CCD at the HPCAT-IDB beamline ($\lambda = 0.39779$ Å) at the Advanced Photon Source (APS) at Argonne National Laboratory, and a MAR345 imaging plate at the B2 beamline ($\lambda = 0.49594$ Å), Cornell High Energy Synchrotron Source (CHESS), Cornell University. The pressure–volume (P – V) data nc-TiO₂ anatase phase was fit by using a second-order Birch–Murnaghan EOS (BM-EOS),²³ where the first pressure derivative of the bulk modulus K_0' is fixed to 4 to more easily compare with previous studies (Table 1). Other details on the experimental methods can be found elsewhere.^{24–26}

Received: July 31, 2012

Revised: September 11, 2012

Published: September 11, 2012

Table 1. The EOSs for nc-TiO₂ Anatase and the Associated Experimental Conditions^a

grain size (nm)	V_0 (Å ³)	K_0 (GPa)	K_0'	pressure range (GPa)	pressure medium	ref	notes
40	34.06(0.04)	198(10)	4	0–11	M-E-W (16:3:1)	this study	
20	34.14(0.05)	169(9)	4	0–11	M-E-W (16:3:1)	this study	
30–40	34.04	243(3)	4	0–16	no medium	ref 10	Nonhydrostatic compression
6	NA	237(3)	4	0–18	fluorinert FC70-FC77 (1:1)	ref 8	Nonhydrostatic compression above ~2.5 GPa
6	34.18	176(15)	4	0–23	M-E-W (16:3:1)	ref 13	- The EOS is not given in this ref - We compute the EOS from the given P – V data - V_0 is determined from the 5 d -spacings given in this ref
		165(9)	4	0–9			
		165(8)	4	0–13			
		168(10)	4	0–17			
		171(12)	4	0–19			
6.5	NA	199(1.5)	NA	0–12	M-E (4:1)	ref 4	- V_0 for the 15 nm grain size is too low and contradicts findings - K_0' is not given in this ref
15	33.81	239(4.8)	NA	0–12			
15	34.14*	245(4.2)	NA	5–12			- The 5–12 GPa for the 15 nm grain size is where our P – V data agree with this ref and we have used our V_0 for the 20 nm size to fit a second-order BM-EOS
		222(12)*	4*				
		200(10)*	12.27*				
4	NA	185(2.6)	NA	NA			
7.2	NA	211(5)	NA	NA			
9	NA	230(5.1)	NA	NA			
13.5	NA	237(1.5)	NA	NA			
21.3	NA	234(2.6)	NA	NA			
24	NA	228(6.3)	NA	NA			
30.1	NA	226(4.6)	NA	NA			
45	NA	215(5.7)	NA	NA			
micro-crystalline	34.07	190(10) 201(21)*	5.3 (0.1) 4*	0–14	M-E-W (16:3:1)	ref 27	

^aThe EOSs were obtained from a second-order BM-EOS²³ (with $K_0' = 4$). For comparison, we list other experimental results.^{4,8,10,13,27} Where the K_0' value is given as 4; this value is fixed for the calculation. 1σ uncertainties are given in parentheses. For values not given, NA is shown. An asterisk indicates a revised EOS, using a second-order BM-EOS.²³

RESULTS AND DISCUSSION

In all experimental runs, nc-TiO₂ anatase was stable up to the maximum pressure in this study of ~11 GPa (Figures 1–3). The sample with 20 nm average particle size shows an ~15% reduction in bulk modulus as compared to the sample with an average particle size of 40 nm (Table 1, Figure 2). Our measured second-order BM-EOS²³ for the 40 nm nc-TiO₂ anatase gives a bulk modulus $K_0 = 198(10)$ GPa with $V_0 = 34.06(0.04)$ Å³/f.u.; whereas for the 20 nm size, we obtain a significantly lower value of $K_0 = 169(9)$ GPa with $V_0 = 34.14(0.05)$ Å³/f.u. (Table 1, Figure 2).

In our study, the bulk moduli of nc-TiO₂ anatase for both sizes are significantly smaller than those reported previously.^{8,10} The reported K_0 values in these studies are 237(3) and 243(3) GPa when K_0' is fixed to 4 for 6 nm⁸ and 30–40 nm¹⁰ grains, respectively (Table 1). Thus, despite the significant grain size difference in these studies,^{8,10} the bulk modulus appears to be almost size independent and much higher than that of the microcrystalline value of ~200 GPa²⁷ (Table 1). However, both studies^{8,10} suffered from nonhydrostatic compression conditions (Figure 2). No pressure medium was used in ref 10, whereas in ref 8, a Fluorinert FC70-FC77 (1:1) mixture was used. In the latter study, the hydrostaticity limit of the pressure

medium does not exceed 2.5 GPa,^{28,29} which is clearly visible as a kink in the corresponding P – V diagram at ~2 GPa (Figure 2a). The nonhydrostatic conditions have an effect on the EOS because of the systematic error introduced in the determined pressure of the material.^{30–32} Additionally, in a comparison with available data on the compressional behavior of nc-TiO₂ anatase for sizes as low as 6 nm^{4,13} (Figure 2a) and for other nc-TiO₂ phases,^{33,34} no such kink is observed. Consequently, nonhydrostaticity is likely responsible for the significant overestimation of the bulk modulus.^{8,10}

A recent study⁴ explored the effect of grain size on nc-TiO₂ anatase on the bulk modulus under hydrostatic conditions and reported a critical size of 15 nm below which K_0 decreases (Table 1, Figure 2b). However, the measured bulk moduli in this study⁴ require further analyses as K_0 obtained from a BM-EOS is very sensitive to both V_0 and K_0' .²³ The reported value of V_0 (Table 1, Figure 2a) is inconsistent with previous measurements of nc-TiO₂ anatase,^{13,35,36} where V_0 increases as grain size decreases; ref 4 finds the opposite behavior. Moreover, K_0' is not reported,⁴ thus a true comparison cannot be made on the size dependence of the bulk modulus (Table 1). However, the P – V data of the 15 nm grains (ref 4) agree with our 20 nm size at $P > 4$ GPa (Figure 2a). Therefore, if we

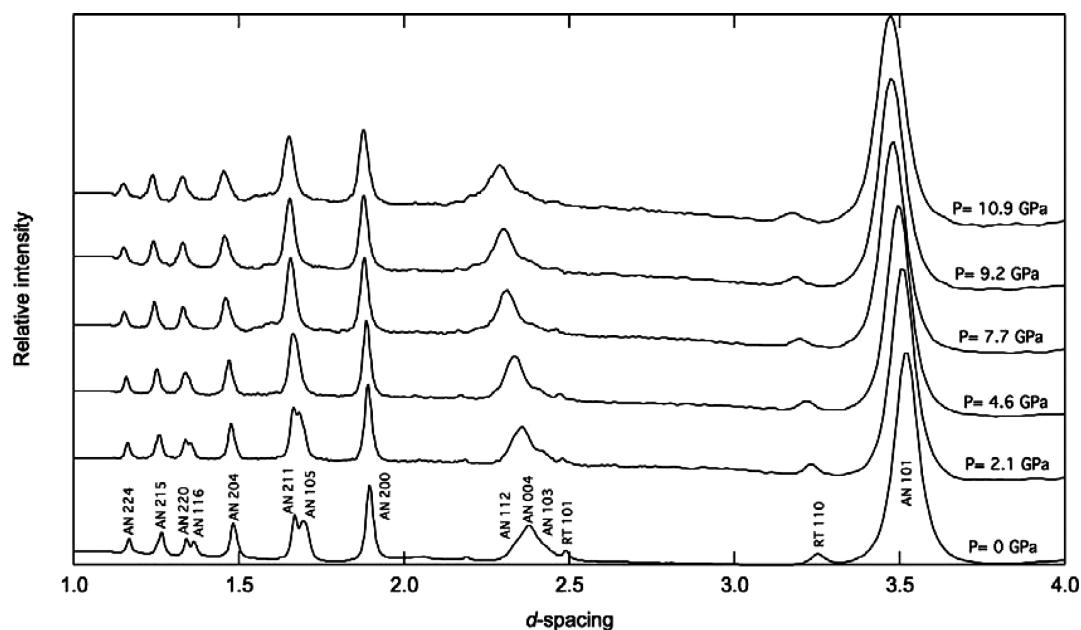


Figure 1. XRD patterns at various pressures during compression of nc-TiO₂ anatase of 20 nm grain size up to 10.9 GPa show the corresponding *hkl* values for anatase (AN) and rutile (RT).

use our $V_0 = 34.14 \text{ \AA}^3$ for the 20 nm size and fit a second-order BM-EOS²³ for the high-pressure data of ref 4 (i.e., for $P > 4$ GPa), we obtain $K_0 = 173(13)$ GPa, in excellent agreement with our measured value (Table 1) and $\sim 28\%$ lower than the reported values in ref 4 of $K_0 = 239\text{--}245$ GPa for the 15 nm grain size. Hence, an increase of V_0 by 1%, for consistency with our study and others,^{13,35,36} leads to a significant reduction of the bulk modulus. On the other hand, if we fit a second-order BM-EOS to the entire pressure range, we obtain a $K_0 = 222$ GPa (Table 1), still an $\sim 8\%$ reduction in comparison to the reported values. The reported K_0 values are 215(5.7) and 234(2.6) GPa for 45 and 21.3 nm average particle size, respectively.⁴ For similar sizes, our bulk moduli are 198(10) and 169(9) GPa (Table 1). Notably, the K_0 value for the 6.5 nm is $\sim 20\%$ higher than the value we compute for the 6 nm size¹³ (Table 1). However, while the data given in ref 4 are insufficient for a detailed reanalysis of the EOSs for each particle size, we suspect that a significant reduction of K_0 , similar to that for the 15 nm particle size, may also occur. Thus, in comparison to ours and another recent study¹³ where hydrostatic conditions are present, K_0' is constrained and V_0 is consistent with previous studies,^{35,36} ref 4 may significantly overestimate K_0 for nc-TiO₂ anatase, which is at least partly due to the choice of K_0' as well as V_0 as discussed above.

In a recent study on the hydrostatic compressional behavior of 6 nm TiO₂ anatase,¹³ we find excellent agreement with our results for the 20 nm grain size (Figure 3, Table 1). In addition to the similar hydrostatic conditions, the larger V_0 value reported in this study is consistent with ours and previous measurements of nc-TiO₂ anatase^{35,36} (Table 1). The change in normalized lattice parameters (a/a_0 and c/c_0) with pressure in ref 13 is also in good agreement with ours (Figure 3b), where c is much more compressible than a . However, the focus of ref 13 was on the unusual compressional behavior of nc-TiO₂ anatase but without an EOS determination. We, thus, have computed the EOS for the 6 nm anatase from ref 13 (Table 1) and find excellent agreement with our measured K_0 for the 20 nm size; the computed value of K_0 has a value of ~ 170 GPa with K_0'

fixed to 4 regardless of the choice of the pressure range used to fit the second-order BM-EOS²³ (Table 1). In detail, $K_0 = 165(9)$ GPa for P -range up to ~ 9 GPa, where the M-E-W pressure medium is still hydrostatic, and $K_0 = 176(15)$ GPa for the whole P -range up to ~ 23 GPa (Table 1). Thus, despite the small kink observed at pressures of 10–12 GPa,¹³ likely due to freezing of M-E-W pressure medium,^{20,21} the bulk moduli are consistent with our value of 169(9) GPa (Table 1). Thus, we conclude that the bulk modulus of anatase does not change for grain sizes between 6 and 20 nm. It has been suggested that at this small grain size, nc-TiO₂ anatase is too small to sustain high dislocation concentrations, which is consistent with the observed reduction of the bulk modulus.⁴ The surface of the nc-TiO₂ particles consists most likely of undersaturated oxygen and/or titanium sites. Therefore, these sites may undergo reactions with the M-E-W pressure medium. However, we do not observe OH⁻ contamination through asymmetry in the XRD peaks and this effect is likely not dominant. An alternative mechanism is that the thickness of the strained surface layer is sufficiently large that it can affect the bulk modulus directly.³⁷ With decreasing particle size we observe an increased effective volume relative to the microcrystalline reference (Table 1) suggesting the presence of an extensive (average) strain. We attribute the unexpectedly large reduction in bulk modulus to a significantly strained outer shell of the particles. Assuming that the thickness of the strained shell depends weakly on the size of the particle, it follows as the volume fraction of the shell relative to the particle volume increases with decreasing particle size that the bulk modulus reduction should become more pronounced. However, if this trend continues for very small particle size, where the energetics of the strained shell may promote restructuring, remains unclear.

The measured bulk modulus of microcrystalline bulk TiO₂ anatase of ~ 200 GPa²⁷ (Table 1) is in good agreement with our K_0 for the 40 nm grain size. Both, ours (40 nm) and previous bulk anatase,²⁷ show similar compressional behavior (Figure 2b). Since the 40 nm anatase behaves like microcrystalline samples, we conclude that the bulk modulus of anatase is size-

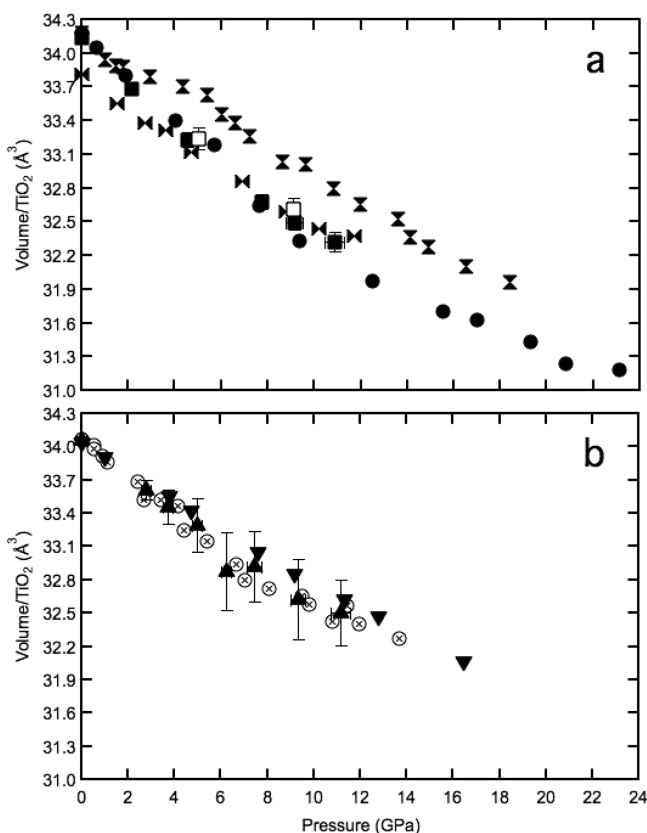


Figure 2. Pressure versus volume of one TiO_2 unit for nanocrystalline anatase for 20 (squares) and 40 nm (triangles) sizes. The solid symbols indicate points under compression, and open symbols indicate points upon decompression. (a) For the 20 nm grain size, our high-pressure volumes are smaller than previous work shown⁸ (vertical bowties). V_0 in ref 8 is not given, thus we assumed the same value as measured by ref 13 for the same grain size. V_0 of 15 nm grain size⁴ (horizontal bowties) is smaller than our V_0 and is inconsistent with V_0 measurements of nc- TiO_2 anatase.^{13,35,36} (b) Our high-pressure volumes are smaller than previous work¹⁰ on 30–40 nm (inverted triangles). The compression behavior of our 40 nm grain size is similar to that of microcrystalline TiO_2 (crossed circles²⁷).

independent for grain sizes larger than ~ 40 nm (Figure 4). On the other hand, for smaller grain sizes we find a much lower K_0 as compared to the 40 nm sample, suggesting that in the size range of 20–40 nm, the compressibility of nc- TiO_2 anatase rapidly changes by $\sim 15\%$ (Figure 4).

The observed decrease in K_0 of TiO_2 anatase as the particle size is reduced is consistent with previous observations for some other oxides and metals (e.g., ZrO_2 ,^{38,39} SnO_2 ,⁴⁰ Al_2O_3 ,⁴¹ MgO ,⁴² ZnO ,⁴³ and Ni ⁴⁴), although this is not a universal behavior (e.g., CuO ⁴⁵ and Fe ⁴⁶ are size-independent, whereas K_0 increases as particle size is reduced in Fe_2O_3 ,⁴⁷ Ag ,⁴⁸ and Au ⁴⁸). We should also note that although the bulk modulus of anatase decreases with grain sizes < 40 nm, this is not necessarily evidence for an inverse Hall–Petch effect,^{49,50} as the bulk modulus is not a good indicator for hardness, instead the shear modulus is a better measure of hardness.^{24,26,51,52} Thus, measurements on the grain size dependence of the shear modulus of nc- TiO_2 anatase are necessary to examine whether anatase follows an inverse Hall–Petch effect or not.

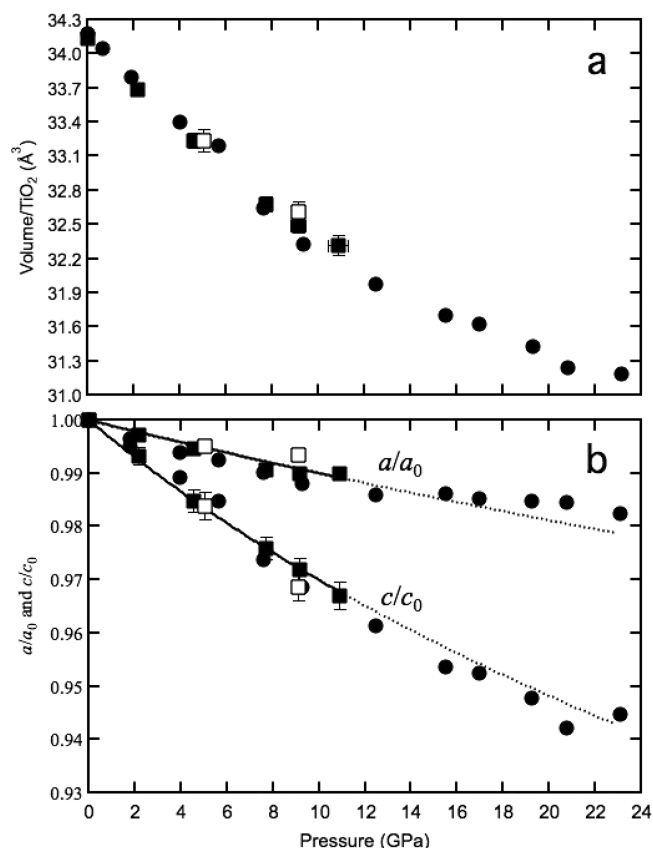


Figure 3. (a) The compression behavior of our 20 nm grain size is in good agreement with the 6 nm size previously observed¹³ (circles). (b) The change in the normalized unit cell parameters (a/a_0 and c/c_0) as a function of pressure. Refer to Figure 2 caption for symbol identification. Solid lines indicate the linear BM-EOS⁵³ for a and c axes up to ~ 11 GPa. The dashed curve is extrapolated from the linear BM-EOS fit⁵³ and shows good agreement beyond the hydrostatic limit of M-E-W as well as with a previous study.¹³

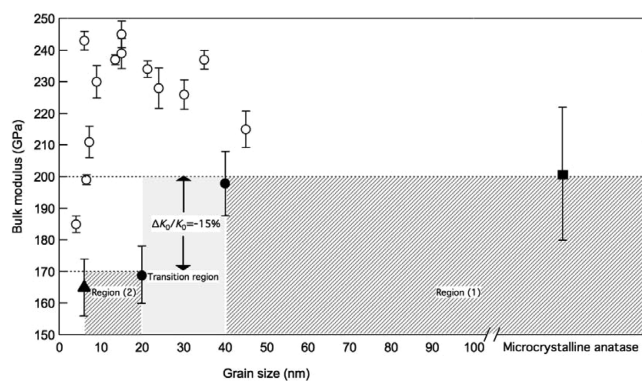


Figure 4. The change in bulk modulus of anatase as a function of grain size. Closed symbols show our values (circles) and those of the microcrystalline TiO_2 anatase (square²⁷) and of 6 nm nc- TiO_2 anatase (triangle¹³). The bulk modulus of anatase is size-independent in, at least, two regions: from microcrystalline size down to 40 nm and from 6 to 20 nm. The region between 20 and 40 nm indicates a transition region for nc- TiO_2 anatase. To compare, we show previously reported values (open circles^{4,8,10}).

CONCLUSIONS

In summary, using powder XRD, we have studied the compressional behavior and the size dependence on the bulk

modulus of nc-TiO₂ anatase. While the grain size dependence of the bulk modulus has been controversial, we provide a consistent understanding for the size dependence of the bulk modulus of anatase: (1) for grain sizes >~40 nm (2) and grain sizes from 6 to 20 nm, the bulk modulus is size independent. Between region (1) and region (2), the bulk modulus decreases by ~15%, indicating a strong dependence of bulk modulus on particle size in the size range between 20 and 40 nm.

AUTHOR INFORMATION

Corresponding Author

*E-mail: yalkhatatbeh@simons-rock.edu.

Notes

The authors declare no competing financial interest.

ACKNOWLEDGMENTS

Portions of this work were performed at HPCAT at the APS, Argonne National Laboratory, and at B2 at CHESS, Cornell University. HPCAT is supported by DOE-BES, DOE-NNSA, NSF, and the W.M. Keck Foundation. APS and CHESS are supported by DOE. We thank beamline scientists Jesse Smith, Zhongwu Wang, Yue Meng, and Stanislav Sinogeikin. We also thank George Amulele for experimental help. Portions of this work were funded by the Carnegie/DOE Alliance Center.

REFERENCES

- (1) Chen, X.; Mao, S. S. *Chem. Rev.* **2007**, *107*, 2891–2959.
- (2) Griffin, K. A.; Pakhomov, A. B.; Wang, C. M.; Heald, S. M.; Krishnan, K. M. *Phys. Rev. Lett.* **2005**, *94*, 157204.
- (3) Valden, M.; Lai, X.; Goodman, D. W. *Science* **1998**, *281*, 1647–1650.
- (4) Chen, B.; Zhang, H.; Dunphy-Guzman, A. K.; Spagnoli, D.; Kruger, M. B.; Muthu, D. V. S.; Kunz, M. *Phys. Rev. B* **2009**, *79*, 125406.
- (5) Flank, A.-M.; Lagarde, P.; Itie, J.-P.; Hearne, G. R. *Phys. Rev. B* **2008**, *77*, 224112.
- (6) Hearne, G. R.; Zhao, J.; Dawe, A. M.; Pischedda, V.; Maaza, M.; Nieuwoudt, M. K.; Kibasomba, P.; Nemraoui, O.; Comins, J. D. *Phys. Rev. B* **2004**, *70*, 134102.
- (7) Machon, D.; Daniel, M.; Pischedda, V.; Daniele, S.; Bouvier, P.; LeFloch, S. *Phys. Rev. B* **2010**, *82*, 140102.
- (8) Pischedda, V.; Hearne, G. R.; Dawe, A. M.; Lowther, J. E. *Phys. Rev. Lett.* **2006**, *96*, 035509.
- (9) Shul'ga, Y. M.; Matyushenko, D. V.; Golshev, A. A.; Shakhrai, D. V.; Molodets, A. M.; Kabachkov, E. N.; Kurkin, E. N.; Domashnev, I. A. *Tech. Phys. Lett.* **2010**, *36*, 841–843.
- (10) Swamy, V.; Dubrovinsky, L. S.; Dubrovinskaia, N. A.; Simionovici, A. S.; Drakopoulos, M.; Dmitriev, V.; Weber, H.-P. *Solid State Commun.* **2003**, *125*, 111–115.
- (11) Swamy, V.; Kuznetsov, A.; Dubrovinsky, L. S.; Caruso, R. A.; Shchukin, D. G.; Muddle, B. C. *Phys. Rev. B* **2005**, *71*, 184302.
- (12) Swamy, V.; Kuznetsov, A.; Dubrovinsky, L. S.; McMillan, P. F.; Prakapenka, V. B.; Shen, G.; Muddle, B. C. *Phys. Rev. Lett.* **2006**, *96*, 135702.
- (13) Swamy, V.; Kuznetsov, A. Y.; Dubrovinsky, L. S.; Kurnosov, A.; Prakapenka, V. B. *Phys. Rev. Lett.* **2009**, *103*, 075505.
- (14) Swamy, V.; Muddle, B. C. *J. Aust. Ceram. Soc.* **2008**, *44*, 1–5.
- (15) Wang, Z.; Saxena, S. K. *Solid State Commun.* **2001**, *118*, 75–78.
- (16) Wang, Z.; Saxena, S. K.; Pischedda, V.; Liermann, H. P.; Zha, C. S. *J. Phys.: Condens. Matter* **2001**, *13*, 8317–8323.
- (17) Wang, Y.; Zhao, Y.; Zhang, J.; Xu, H.; Wang, L.; Luo, S.; Daemen, L. L. *J. Phys.: Condens. Matter* **2008**, *20*, 125224.
- (18) Guinier, A. *X-Ray Diffraction In Crystals, Imperfect Crystals, and Amorphous Bodies*; Dunod: Paris, France, 1956.
- (19) Fujishiro, I.; Piermarini, G. J.; Block, S.; Munro, R. G. In *Proceedings of the 8th AIRAPT Conference*; Backman, C. M.,

Johannisson, T.; Tenger, L., Eds.; ISBN: Uppsala, Sweden, 1982; Vol. II, p 608.

(20) Angel, R. J.; Bujak, M.; Zhao, J.; Gatta, G. D.; Jacobsen, S. D. *J. Appl. Crystallogr.* **2007**, *40*, 26–32.

(21) Klotz, S.; Chervin, J.-C.; Munsch, P.; Marchand, G. L. *J. Phys. D: Appl. Phys.* **2009**, *42*, 075413.

(22) Mao, H. K.; Xu, J.; Bell, P. M. *J. Geophys. Res.* **1986**, *91*, 4673–4676.

(23) Birch, F. *J. Geophys. Res.* **1952**, *57*, 227–234.

(24) Al-Khatatbeh, Y.; Lee, K. K. M.; Kiefer, B. *Phys. Rev. B* **2010**, *82*, 144106.

(25) Al-Khatatbeh, Y.; Lee, K. K. M.; Kiefer, B. *Phys. Rev. B* **2009**, *79*, 134114.

(26) Al-Khatatbeh, Y.; Lee, K. K. M.; Kiefer, B. *Phys. Rev. B* **2010**, *81*, 214102.

(27) Arlt, T.; Bermejo, M.; Blanco, M. A.; Gerward, L.; Jiang, J. Z.; Olsen, J. S.; Recio, J. M. *Phys. Rev. B* **2000**, *61*, 14414.

(28) Sidorov, V. A.; Sadykov, R. A. *J. Phys.: Condens. Matter* **2005**, *17*, S3005–S3008.

(29) Varga, T.; Wilkison, A. P.; Angel, R. J. *Rev. Sci. Instrum.* **2003**, *74*, 4564–4566.

(30) Kenichi, T. *Phys. Rev. B* **2004**, *70*, 012101.

(31) Otto, J. W.; Vassiliou, J. K.; Frommeyer, G. *J. Synchrotron Radiat.* **1997**, *4*, 155–162.

(32) Chai, M.; Brown, J. M. *Geophys. Res. Lett.* **1996**, *23*, 3539.

(33) Olsen, J. S.; Gerward, L.; Jiang, J. Z. *High Pressure Res.* **2002**, *22*, 385–389.

(34) Swamy, V.; Dubrovinsky, L. S.; Dubrovinskaia, N. A.; Langenhorst, F.; Simionovici, A. S.; Drakopoulos, M.; Dmitriev, V.; Weber, H.-P. *Solid State Commun.* **2005**, *134*, 541–546.

(35) Ahmad, M. I.; Bhattacharya, S. S. *Appl. Phys. Lett.* **2009**, *95*, 191906.

(36) Swamy, V.; Menzies, D.; Muddle, B. C.; Kuznetsov, A.; Dubrovinsky, L. S.; Dai, Q.; Dmitriev, V. *Appl. Phys. Lett.* **2006**, *88*, 243103.

(37) Sevostianov, I.; Kachanov, M. *Int. J. Solids Struct.* **2007**, *44*, 1304–1315.

(38) Bouvier, P.; Djurado, E.; Lucazeau, G.; Bihan, T. L. *Phys. Rev. B* **2000**, *62*, 8731–8737.

(39) Ohtaka, O.; Fukui, H.; Funakoshi, K.; Utsumi, W.; Irifune, T.; Kikegawa, T. *High Pressure Res.* **2002**, *22*, 221–226.

(40) He, Y.; Liu, J. F.; Chen, W.; Wang, Y.; Wang, H.; Zeng, Y. W.; Zhang, G. Q.; Wang, L. N.; Liu, J.; Hu, T. D.; et al. *Phys. Rev. B* **2005**, *72*, 212102.

(41) Chen, B.; Penwell, D.; Benedetti, L. R.; Jeanloz, R.; Kruger, M. B. *Phys. Rev. B* **2002**, *66*, 144101.

(42) Marquardt, H.; Gleason, A.; Marquardt, K.; Speziale, S.; Miyagi, L.; Wenk, H.-R.; Jeanloz, R. *Phys. Rev. B* **2011**, *84*, 064131.

(43) Jiang, J. Z.; Olsen, J. S.; Gerward, L.; Frost, D.; Rubie, D.; Peyronneau, J. *Europhys. Lett.* **2000**, *50*, 48–53.

(44) Zhang, J.; Zhao, Y.; Palosz, B. *Appl. Phys. Lett.* **2007**, *90*, 043112.

(45) Wang, Z.; Pischedda, V.; Saxena, S. K.; Lazor, P. *Solid State Commun.* **2002**, *121*, 275–279.

(46) Chen, B.; Penwell, D.; Kruger, M. B.; Yue, A. F.; Fultz, B. *J. Appl. Phys.* **2001**, *89*, 4794–4796.

(47) Jiang, J. Z.; Olsen, J. S.; Gerward, L.; Morup, S. *Europhys. Lett.* **1998**, *44*, 620–626.

(48) Gu, Q. F.; Krauss, G.; Steurer, W.; Gramm, F.; Cervellino, A. *Phys. Rev. Lett.* **2008**, *100*, 045502.

(49) Hall, E. O. *Proc. Phys. Soc., London, Sect. B* **1951**, *64*, 747.

(50) Petch, N. J. *J. Iron Steel Inst., London* **1953**, *174*, 25.

(51) Haines, J.; Leger, J. M.; Bocquillon, G. *Annu. Rev. Mater. Res.* **2001**, *31*, 1–23.

(52) Teter, D. M. *MRS Bull.* **1998**, *23*, 22–27.

(53) Xu, H.; Zhao, J.; Zhang, J.; Wang, Y.; Hickmott, D. D.; Daemen, L. L.; Hartl, M. A.; Wang, L. *Am. Mineral.* **2010**, *95*, 19–23.